Materials Engineering Lab.

Reaction and Excitation Dynamics Group

(Japanese)

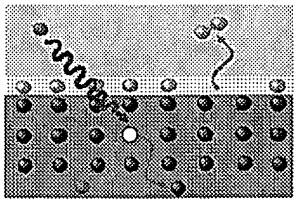

SCOPE

Femtosecond- and atomic-scale control over reaction on surfaces and interfaces is essential for developing materials for nanoscale ultrafast devices. We are investigating the femtosecond excitation and relaxation dynamics of carriers and phonons in solids, the energy transfer during reactions between atoms/molecules and surfaces, and the surface stress during film growth and defect formation.

keywords: coherent phonon, vibrational and rotational states, surface stress.

TOPICS

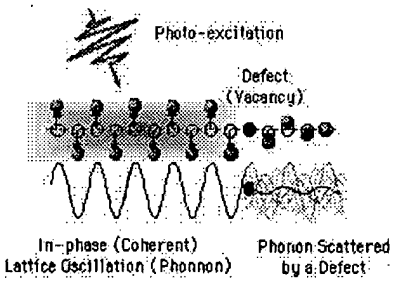

Femtosecond Phonon Dynamics

Femtosecond light pulses excite coherent lattice oscillations (phonons) as well as non-equilibrium carriers in semiconductors and metals. The excited carriers and phonons relax in subpico- and picosecond time scates due to carrier-carrier, carrier-phonon and defect scatterings. These ultrafast relaxation dynamics are crucial in developing materials for ultrafast devices.
We are studying the relaxation of coherent phonons and carriers in defective semiconductors and semimetals by means of pump-probe reflectivity measurements to search possibilities of controlling the relaxation dynamics by introduction of vacancies into materials.

Reactive Scattering of Molecular/Atomic Beams with Surfaces

Reactive scattering dynamics of molecules/atoms by surfaces is complex even for a simple system such as H/Si, because there are many degrees of freedom for energy re-distribution. We have developed an intense atomic hydrogen source and time-of-flight detection system to investigate the translational energy of molecules desorbed from the surface. The internal (vibrational and rotational) states of the molecules are selected by resonance enhanced multi-photon ionization (REMPI) technique.

Surface Stress of Silicon

Stresses at surfaces and interfaces are very crucial for reliability of nanoscale devices. We have constructed a high-sensitive real-time detection system of the surface stress of silicon based on optical micromechanical chantilever technique, and observed very small changes in the surface stress during molecular adsorption/ desorption, ultrathin oxide growth, and disordering of crystalline surfaces.

Phonon Localization in Solids under Ion Irradiation

Raman spectra of crystals is modified by introduction of disorder. The modification is explained by the spatial correlation (SC) model. The degree of disorder is estimated quantitatively in terms of the phonon correlation length, L, which corresponds to a size of phonon confinement by microcrystalline size or by defects. Using this model, we have studied the kinetics of disordering of graphite and semiconductors under ion irradiation and its thermal relaxation.

Hydrogen Molecules in Silicon (collaborating with Prof. Murakami's Lab at Univ. Tsukuba)

Defects in Crystals Studied by Raman Scattering

(Japanese)

III. Kinetic Study on Lattice Disordering

2. Graphite

Because of the existence of the disorder-induced Raman scattering peak, the Raman spectrum of graphite is very sensitive to lattice disorder. The first real-time Raman measurements were therefore carried out on graphite.

Figure 4 shows the first real-time observation of highly oriented pylolytic graphite (HOPG) under ion irradiation. Only the Raman peak of the E_{2g2} optical phonon is observed at 1580 cm^{-1} before irradiation. Irradiation of 3 keV He^+ induces a peak at 1360 cm^{-1} (D). The D-peak grows in height under ion irradiation. A broad asymmetric Raman band centered around 1500 cm^{-1} which is characteristic to amorphous is not observed in this fluence range.

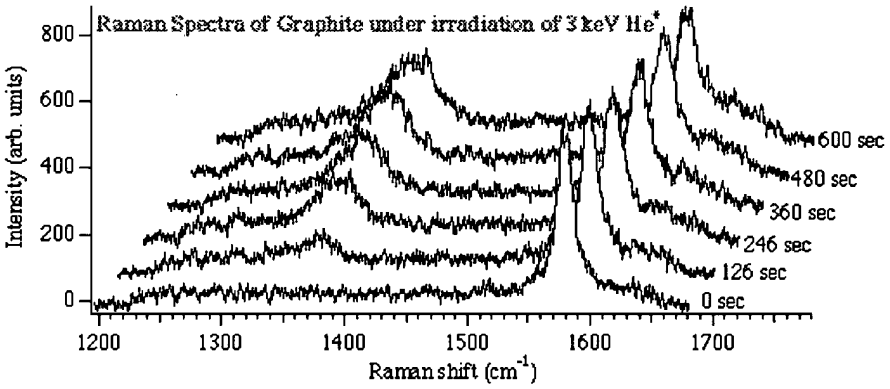

Fig. 4 Raman spectra of highly oriented pylolytic graphite (HOPG) under irradiation of 3 keV He^+ at a flux of 2.0 x 10^{11} $He/cm^2/s$. The peak at 1580 cm^{-1} is the Raman active E_{2g2} mode, and that at 1360 cm^{-1} is a disorder-induced (D-) peak.

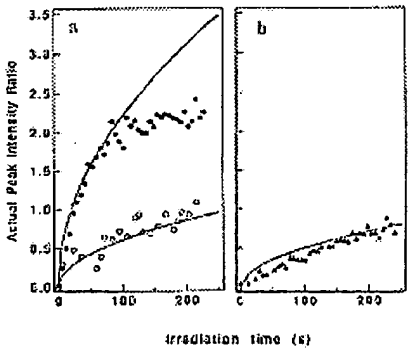

Fig. 5 Time evolution of the relative intensity R of the D-peak to the E_{2g2} peak of graphite under irradiation of (a) 3 keV Ar^+ at fluxes of 2.5 x 10^{11} $/cm^2s$ (solid circle) and 3.3 x 10^{10} $/cm^2s$ (open circle) and (b) 3 keV He^+ at a flux of 2.0 x 10^{11} $/cm^2s$ (solid triangle). Solid curves are the results of calculation with the IDD model.

The fluence applied here is 10^{13} ions/cm^2 at most. In this fluence range, only very local defects are created in graphite planes. Then the average number density of vacancies per volume N_V is given by

$$N_V=N\sigma\nu\varphi t$$

where N is the density of the target atom (1.25×10^{23} atoms/cm^3 for graphite), σ the displacement cross section, φ is the incident ion flux, ν the damage function, *i.e.*, the mean number of displaced atoms in the cascade per primary knock-on, and t the duration of irradiation.

In two-dimensional crystal such as graphite, the areal density N_A of vacancies gives better estimation of disorder;

$$N_A=Nf\sigma\nu\varphi t$$

where f is the distance between graphite layers (0.335 nm). The mean distance between vacancies in a plane L_V is given by

$$L_V=N_A^{-1/2}=(Nf\sigma\nu\varphi t)^{-1/2}$$

Since the vacancies cut the interaction between lattice atoms, **L_V is expected to equal to the in-plane phonon correlation length L**. This is called "**inter-defect distance (IDD) model**" and schematically illustrated in Fig. 6. The intensity ratio of the Raman peaks from L_V is then expressed by

$$R=4.4/L=4.4/L_v=4.4(Nf\sigma\nu\varphi t)^{1/2}=\alpha(\varphi t)^{1/2}$$

The above equation explains the square-root dependence of the relative intensity R on the duration of the irradiation t. The displacement cross section σ and the damage function ν are calculated after Sigmund [5] and Kinchin-Pease [6], respectively. The calculated relative intensity is shown in Fig. 5. It reproduces very well the experimental data for both Ar^+ and He^+ irradiation. The deviation from the calculation at longer times is explained by aggregation and clustering of vacancies.

The disordering rate α is not significantly dependent on ion energies in the keV range, since the product ($\nu \times \sigma$) does not change much as the ion energy increases. Actually, the disordering rate constant obtained experimentally under He^+ irradiation was almost the same for all ion energies of (0.5-5 keV). [7]

A systematic study on ion-mass dependence of on the disordering rate α was performed. The intensity ratio R was increased proportionally to the square root of the duration of the irradiation time also for Ne^+, Kr^+, and Xe^+ ions. α increases as the ion mass increases as shown in Fig. 7.

The calculation with IDD model with parameters listed in Table 1 reproduces the experimental values well. The agreement suggests that the in-plane phonon correlation length L is equal to the mean distance between defects L_V in the graphite plane in the initial stage of ion irradiation. This implies that single vacancies terminate the spatial extension optical phonon in graphite plane.

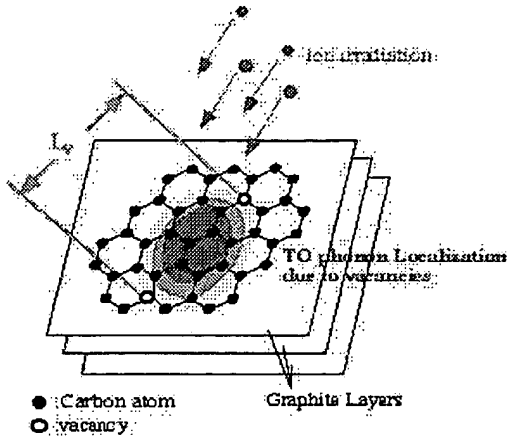

Fig. 6 Schematic illustration of phonon localization due to vacancies in graphite according to inter-defect distance (IDD) model.

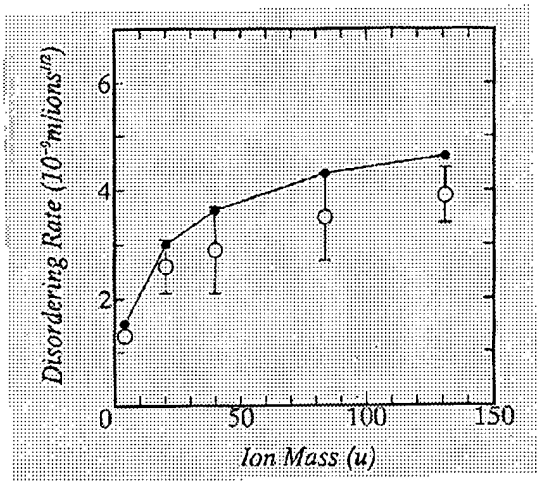

Fig. 7 Ion-mass dependence of the disordering rate α of graphite: experimental results (circle) and calculated values from IDD model (solid circle).

Table 1 Calculated displacement cross section σ, calculated damage function *n*, and experimental and calculated disordering rate α.

Ion	ν	$\sigma(10^{-21}m^2)$	$\alpha_{exp}(10^{-9}m/ions^{1/2})$	$\alpha_{calc}(10^{-9}m/ions^{1/2})$
3 keV He^+	2.32	1.25	1.3+/-0.1	1.53
3 keV Ne^+	2.43	4.59	2.6+/-0.3	3.01
3 keV Ar^+	2.29	7.12	2.9+/-0.8	3.64
3 keV Kr^+	2.05	11.1	3.8+/-0.5	4.30
3 keV Xe^+	1.87	14.1	4.1+/-0.1	4.62

[4] Nakamura, K., and Kitajima, M., *Appl. Phys. Lett.* **59**, 1550, 1991; *Phys. Rev.* **B 45**, 78, 1992; *Phys. Rev.* **B 45**, 5672, 1992.
[5] Sigmund, P., in Sputtering by Particle Bombardment I, ed by Behrish, R., Springer, Berlin, 9, 1981.
[6] Kinchin, G, H., and Pease, R, S., *Rep. Prog. Phys.* **18**, 1, 1955.
[7] Nakamura, K, G., Asari, E., and Kitajima, M., *J. Nucl. Mater.* **187**, 294, 1992.
[8] Asari, E., Kamioka, I., Nakamura, K. G., Kawabe, T., Lewis, W. A., and Kitajima, M., *Phys. Rev.* **B 49**, 1011, 1994.

[Raman Top] / [Home]